

Biofouling Effects on the Response of a Wave Measurement Buoy in Deep Water

JIM THOMSON, JOE TALBERT, ALEX DE KLERK, ADAM BROWN, AND MIKE SCHWENDEMAN

Applied Physics Laboratory, University of Washington, Seattle, Washington

JARETT GOLDSMITH

DNV GL, San Diego, California

JULIE THOMAS, COREY OLFE, AND GRANT CAMERON

Coastal Data Information Program, Scripps Institution of Oceanography, University of California, San Diego, La Jolla, California

CHRISTIAN MEINIG

Pacific Marine Environmental Laboratory, National Oceanic and Atmospheric Administration, Seattle, Washington

(Manuscript received 9 February 2015, in final form 17 March 2015)

ABSTRACT

The effects of biofouling on a wave measurement buoy are examined using concurrent data collected with two Datowell Waveriders at Ocean Station *P*: one heavily biofouled at the end of a 26-month deployment, the other newly deployed and clean. The effects are limited to the high-frequency response of the buoy and are correctly diagnosed with the spectral “check factors” that compare horizontal and vertical displacements. A simple prediction for the progressive change in frequency response during biofouling reproduces the check factors over time. The bulk statistical parameters of significant wave height, peak period, average period, and peak direction are only slightly affected by the biofouling because the contaminated frequencies have very low energy throughout the comparison dataset.

1. Introduction

Wave measurement buoys are moored throughout the world’s oceans for research, maritime safety, and recreational information. Most wave buoys use the heave, pitch, and roll of the buoy to calculate the bulk statistics of the waves (e.g., significant wave height, peak period), the scalar wave energy frequency spectra, and the directional moments of the frequency spectra (Kuik et al. 1988). More recently, wave buoys using the phase-resolved velocities of global positioning system (GPS) receivers are becoming common (Herbers et al. 2012; Thomson 2012). All types of wave buoys rely on the

wave-following nature of the buoy to provide accurate measurements of the moving sea surface. Here, we examine a case of severe biofouling on a wave buoy and the resulting effects on the hydrodynamic response of the buoy (and thus the fidelity of the wave measurements).

A wave measurement buoy must respond to surface motions at all frequencies f of interest (Middleton et al. 1977). In the open ocean, this range is approximately $0.05 < f < 0.5$ Hz (equivalent to wave periods $20 < T < 2$ s). A simplistic approach to the hydrodynamics of a floating body is to consider the heave response frequency f_{hr} , which is the shortest time scale that a floating body can respond to changes in the sea surface elevation. This is given by (Hudspeth 2006)

$$f_{hr} = \frac{1}{2\pi} \sqrt{\frac{F_B g}{ML}}, \quad (1)$$

where $F_B = \rho_{sw} V$ is the buoyancy (from the displacement volume V of seawater with density ρ_{sw}), g is

 Denotes Open Access content.

Corresponding author address: Jim Thomson, Applied Physics Laboratory, University of Washington, 1013 NE 40th Street, Box 355640, Seattle, WA, 98105-6698.
E-mail: jthomson@apl.washington.edu

DOI: 10.1175/JTECH-D-15-0029.1

gravity, M is the mass (including added mass), and L is the vertical length (or draft) of the body. Wave buoys typically have very high response frequencies ($f_{hr} > 1$ Hz) and respond well to wave motions at all frequencies less than this value. Larger bodies (e.g., ships) have lower response frequencies and thus do not respond to high-frequency waves. Changes in the water plane area with draft provide corrections to the buoyancy F_B , but the simplified version is sufficient for the analysis that follows.

Heave response is sufficient for scalar wave measurements of wave energy spectra and associated bulk parameters of significant wave height, peak period, and energy-weighted average period. A directional wave measurement buoy, by contrast, must respond to both vertical and horizontal wave motions. Datawell directional buoys return “check factors” for each frequency band in the wave spectra. These are the ratio of horizontal displacements to vertical displacements,

$$ck(f) = \frac{XX(f) + YY(f)}{ZZ(f)}, \quad (2)$$

which are unity for perfectly circular wave orbits in deep water (Mei 1989). At frequencies above the response frequency, the buoy cannot respond fast enough in heave. At these high frequencies, vertical motions become muted relative to the horizontal displacements, leading to $ck(f) > 1$. Therefore, if the response frequency of the buoy is reduced, as biofouling changes the mass M or size L , then one might expect an increase in the check factor at high frequencies.

2. Observations

The Applied Physics Laboratory at the University of Washington (APL-UW), in cooperation with the Pacific Marine Environmental Laboratory at the National Oceanic and Atmospheric Administration (PMEL-NOAA), has maintained a wave buoy at Ocean Station P since June 2010. Ocean Station P has been an ocean reference station in the North Pacific (50°N , 145°W) since World War II (Freeland 2007). The wave measurements support the broad community of researchers working at this site and are incorporated into the Coastal Data Information Program (CDIP) as station 166 and the National Data Buoy Center (NDBC) as station 46246.

The complete mooring is shown in Fig. 1 and consists of a Datawell Directional Waverider MKIII 0.9-m-diameter buoy at the surface, a “false bottom” created by two steel floats at 150 m below the surface, and an anchor at 4250-m depth. The waverider is connected to the false bottom with a 30-m rubber cord and

300 m of line, such that the upper section is slack and allows the buoy to follow the surface wave motions.

The mooring was first deployed from the R/V *Tully* in June 2010, then subsequently replaced in October 2012 from the R/V *New Horizon*, and again in January 2015 from the R/V *T. G. Thompson*. As shown in Fig. 2 with comparative images, the buoy deployed in October 2012 was newly painted with yellow marine paint (PPG Amercoat). When the same buoy was recovered in January 2015, it was severely biofouled with gooseneck barnacles (*Lepas anatifera*). Using a simple marine paint, as opposed to an antifouling paint, was a poor choice made when the 2012 turnaround was rescheduled under very short notice. The replacement buoy deployed in Jan 2015 has an antifouling coating of “E-paint.”

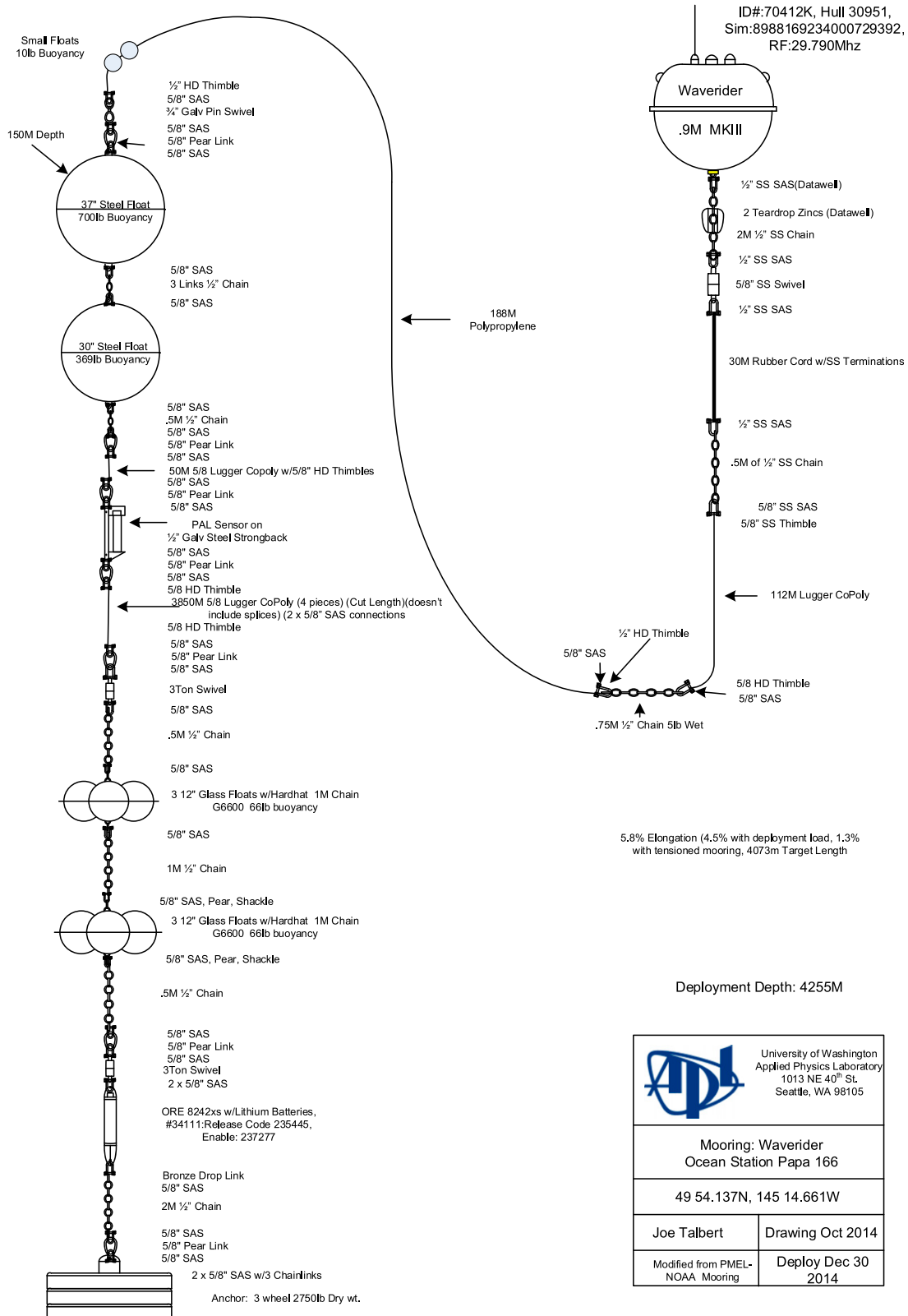
The mooring work during the recent 2015 cruise on the R/V *T. G. Thompson* was sequenced to deploy the replacement mooring first and then recover the existing mooring. Weather and other operations introduced a delay between the mooring operations. This schedule resulted in 42 h of overlapping data, when both the old (fouled) waverider and the new (clean) waverider were deployed simultaneously in close proximity. The time series of bulk parameters during this overlap is shown in Fig. 3. The buoys are approximately 20 km apart, which is necessary for safe mooring operations at such a deep site (4250 m).

The raw data on board the waverider are collected at 1.28 Hz for 30-min bursts and then frequency spectra are calculated on board the waverider buoy using eight 200-s-long windows with no overlap, resulting in spectra with 0.01-Hz frequency resolution and 16 degrees of freedom (a measure of statistical quality).

The response frequency [Eq. (1)] of the clean waverider buoy is $f_{hr} = 1$ Hz, based on a mass of $M_0 = 225$ kg, a displaced volume of that is half of the buoy (waterline is at maximum circumference, thus $V_0 = (1/2)[(4/3)\pi(D/2)^3] = 0.425 \text{ m}^3$), and a half-diameter draft $L_0 = 0.45$ m. This is appropriately well above the wave frequencies analyzed in the waverider’s onboard processing.

3. Analysis

The bulk wave parameters from the two buoys are shown as a time series in Fig. 3. They agree well; however, the direct comparison of significant wave heights in Fig. 4 does show a statistically significant bias for lower wave heights from the fouled buoy. The slope of the least squares regression is 0.96 ± 0.02 , using 95% confidence intervals. Some of the discrepancies and scatter between the two buoys likely are the result of statistical uncertainty in measuring waves from finite-length records. For the 10-s waves observed during the overlapping deployments, each mooring will measure approximately 180



 University of Washington Applied Physics Laboratory 1013 NE 40 th St. Seattle, WA 98105	
49 54.137N, 145 14.661W	
Joe Talbert	Drawing Oct 2014
Modified from PMEL- NOAA Mooring	Deploy Dec 30 2014

FIG. 1. Schematic diagram of the waverider mooring at Ocean Station P (50°N, 145°W; depth: 4250 m).

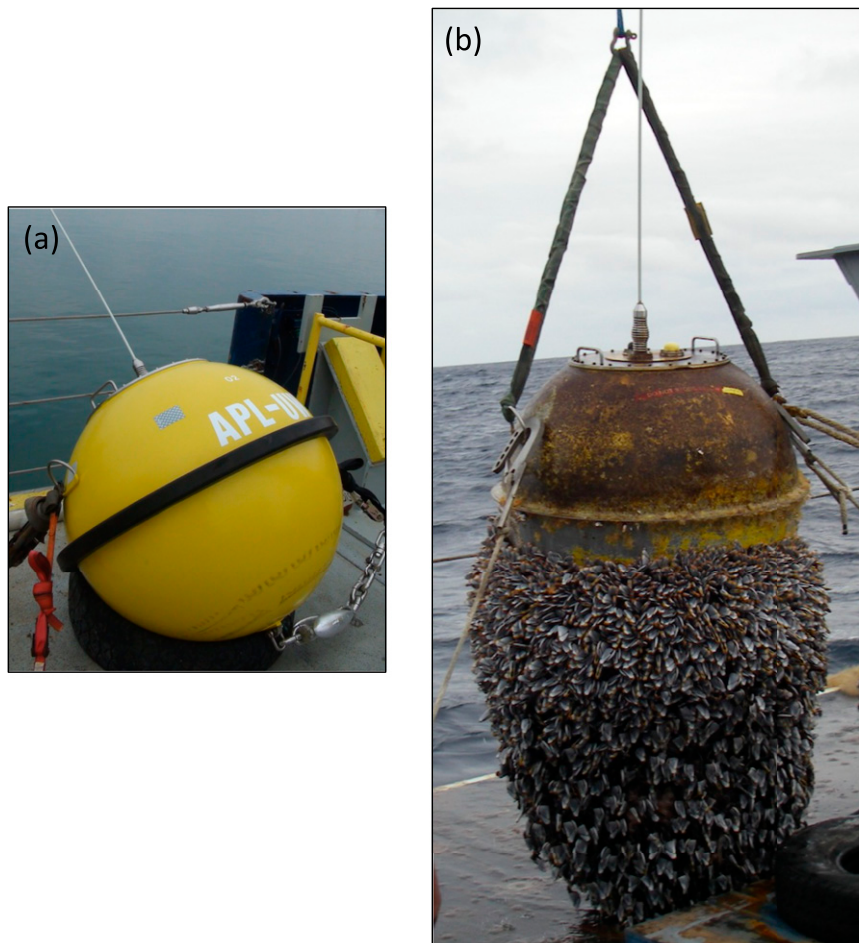


FIG. 2. Before and after pictures of the 0.9-m-diameter waverider buoy at Ocean Station P. (a) Newly painted buoy on deck before deployment in October 2012, and (b) biofouled buoy after recovery in January 2015.

individual waves during a 30-min burst. However, because of the 20-km separation of the moorings, individual waves measured will be different, and thus statistical variation is expected even though spatial variation in the sea state is negligible.

The statistical variations across 30-min records can be mitigated by using 3-h records, and this comparison is also shown in Fig. 4. The bias slope is the same (0.96), and the correlation coefficient is improved from $R^2 = 0.74$ for the short records to $R^2 = 0.93$ for the longer records. This consistent bias indicates that the fouled buoy measures slightly less wave motion than the clean buoy.

The effect of biofouling is most apparent when comparing the spectral response of the buoys. Figure 5 shows the scalar wave energy spectra and the check factors [Eq. (2)] from both buoys during the simultaneous measurements. The clean buoy has a clear f^{-4} shape at high frequencies, which is termed the equilibrium range (Phillips 1985) and is a well-documented feature of ocean surface

waves (e.g., Thomson et al. 2013). The fouled buoy has a muted response at these frequencies, and the spectral slope is much steeper than the expected f^{-4} . This suggests that the fouled buoy is not responding fully to wave motions at these frequencies. Although this is clear in the spectra, it does not have much effect on the bulk parameters (significant wave height, peak period, etc.) because the energy at these frequencies is very low relative to the peak of each spectrum. These spectra are typical of open ocean sites, where swells dominate.

The spectral check factors in Fig. 5 confirm the changes in buoy response as a result of the fouling. Ideally, the check factors are equal to one, indicating perfectly circular orbital motion. For the attenuated high frequencies of the fouled buoy, the check factor is 2 or higher, indicating that the horizontal displacements are at least twice the vertical displacements. The check factors also deviate from unity for the lowest frequencies (low-amplitude swells), which is a known problem in

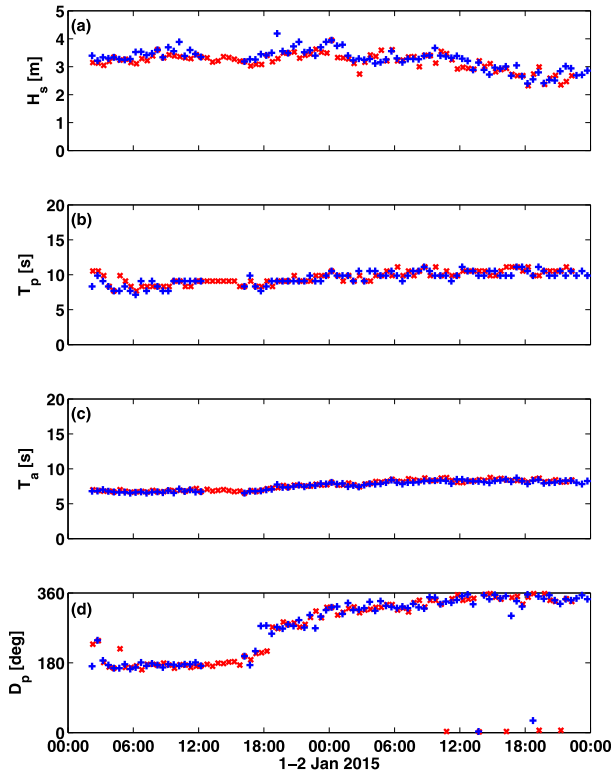


FIG. 3. Time series comparison of (a) significant wave height, (b) peak period, (c) average period, and (d) peak direction from two waveriders deployed simultaneously at Ocean Station P. Red symbols are the biofouled buoy and blue symbols are the clean buoy.

sensor response that is the same for both the fouled and clean buoys.

The high-frequency changes are consistent with the hydrodynamic effects of fouling: by effectively increasing the size and mass of the buoy, the response frequency of the buoy is reduced and the buoy no longer tracks high-frequency changes in the sea surface elevation [Eq. (1)]. In addition to changes in the heave response, the drag of the buoy is likely increased, changing the response to horizontal motions. In the simple model that follows, we restrict analysis to the heave response as the dominant change from biofouling.

Biofouling model

Unfortunately, the biofouling was not weighed upon recovery of the buoy; this was beyond the scope of both the research cruise and the equipment on board. Estimates for the final values of additional volume $V_{bf} = 1 \text{ m}^3$ and draft $L_{bf} = 1.5 \text{ m}$ are used, based on visual comparison (see Fig. 2) with clean buoy values of $V_0 = (1/2)0.85 \text{ m}^3$ and $L_0 = (1/2)0.9 \text{ m}$. The resulting final response frequency at the time of recovery is $f_{hr,bf} \sim 0.35 \text{ Hz}$. This is consistent with the frequency at which the observed spectra deviate

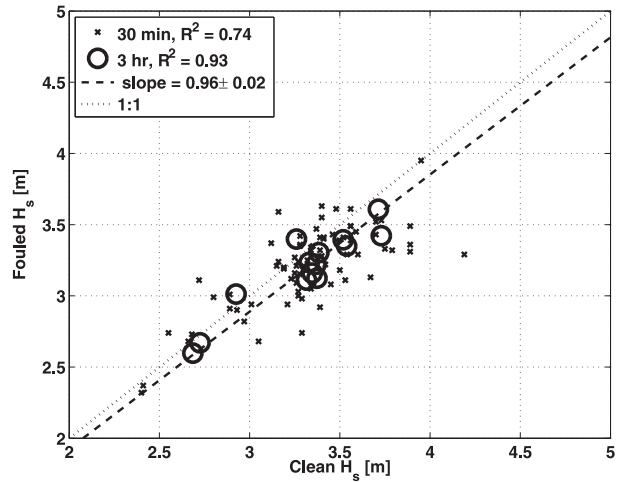


FIG. 4. Direct comparison of significant wave heights from the biofouled buoy vs the clean buoy. Crosses are 30-min records and circles are 3-h records. Both have a regression slope of 0.96.

from the canonical f^{-4} and when the check factors deviate from one (Fig. 5).

The final biofouling values are used in a simple prediction for the time evolution of the frequency response throughout the deployment. Standards for biofouling of moorings and marine hardware suggest that biofouling mass grows linearly for the first 2 years of a deployment and that the biofouling has a density of $\rho_{bf} = 1325 \text{ kg m}^{-3}$ (DNV GL 2014, section 6.7.4). Using this assumption, and the visual guess at the final values for the biofouling, the time evolution of the changing heave response frequency can be estimated from Eq. (1) as

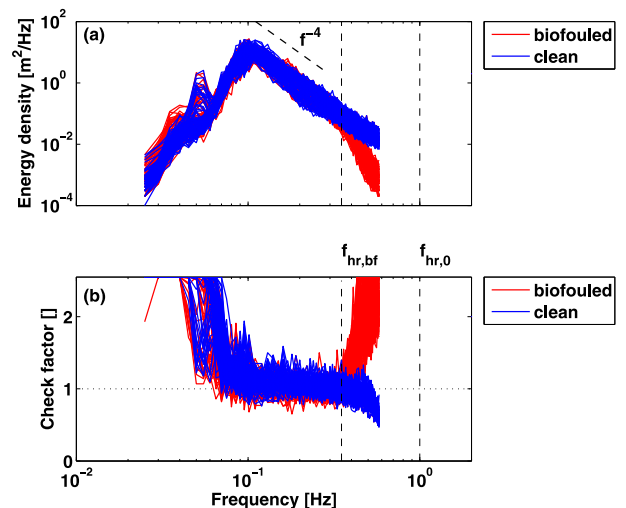


FIG. 5. (a) Wave energy vs frequency and (b) orbital check factor vs frequency. Clean and biofouled response frequencies are shown with vertical dashed lines. Predicted f^{-4} slope of the equilibrium range is also shown with a dashed line.

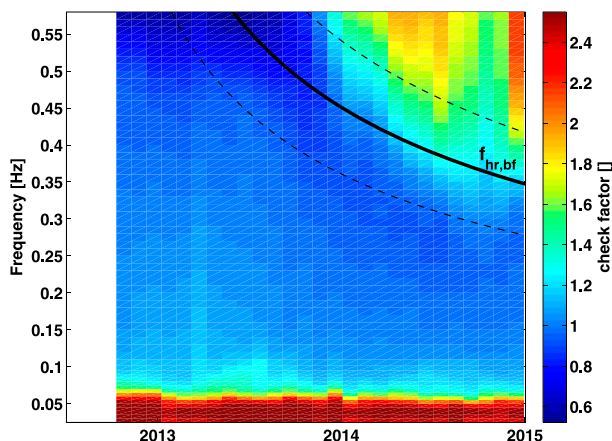


FIG. 6. Spectrogram of check factors (color scale) through time. The black curve is the predicted shift in the response frequency of the waverider assuming linear accumulation of biofouling. The dashed curves represent the 20% uncertainty in the predicted shift of the response frequency, as estimated from the uncertainty in the input parameters.

$$f_{\text{hr}}(t) = \frac{1}{2\pi} \sqrt{\frac{\rho_{\text{sw}} \left[\frac{1}{2} V_0 + V_{\text{bf}}(t) \right] g}{[M_0 + \rho_{\text{bf}} V_{\text{bf}}(t)][L_0 + L_{\text{bf}}(t)]}}. \quad (3)$$

This prediction is validated against the measured time evolution of the spectral check factors in Fig. 6. The prediction successfully identifies the range of contaminated frequencies and the expansion in time of those frequencies.

Figure 6 suggests that Eq. (3) can serve as a simple predictor of contaminated frequencies, given a temporal model for biofouling. There is ample uncertainty in the biofouling model and in the final values for V_{bf} and L_{bf} , as reflected in the 20% error bars shown on the predicted response frequency in Fig. 6. The significant result here, however, is in capturing the degrading frequency response through time, not the exact values.

4. Discussion and conclusions

Many other examples of biofouling effects on wave measurement buoys are documented online (at http://cdip.ucsd.edu/?nav=documents&sub=index&units=metric&tz=UTC&pub=public&map_stati=1,2,3&xitem=check_factor). This example is unique because two waveriders

(one fouled, one cleaned) were deployed simultaneously for 42 h and directly compared. Despite severe biofouling, the effects are limited to the high-frequency response of the buoy. Bulk statistics are mostly unaffected by the biofouling because the attenuated frequencies have very little energy. Thus, biofouling may be primarily a concern for researchers using wave measurements to infer wave dynamics and not a concern for operational users. However, at sites dominated by short wind waves, such as marginal seas, large lakes, and fjords, biofouling may affect the dominant frequencies. In all cases, the spectral check factors are a useful tool in remotely diagnosing the contamination by biofouling.

Acknowledgments. We thank the captains and crews of the R/V *Tully*, R/V *New Horizon*, and R/V *T. G. Thompson*. Funding was provided by the National Science Foundation.

REFERENCES

- DNV GL, 2014: Environmental conditions and environmental loads. Recommend Practice DNV-RP-C205, 182 pp.
- Freeland, H., 2007: A short history of Ocean Station Papa and Line P. *Prog. Oceanogr.*, **75**, 120–125, doi:10.1016/j.pocean.2007.08.005.
- Herbers, T. H. C., P. F. Jessen, T. T. Janssen, D. B. Colbert, and J. H. MacMahan, 2012: Observing ocean surface waves with GPS-tracked buoys. *J. Atmos. Oceanic Technol.*, **29**, doi:10.1175/JTECH-D-11-00128.1.
- Hudspeth, R. T., 2006: *Waves and Wave Forces on Coastal and Ocean Structures*. Advanced Series on Ocean Engineering, Vol. 21, World Scientific, 952 pp.
- Kuik, A. J., G. Ph. van Vledder, and L. H. Holthuijsen, 1988: A method for the routine analysis of pitch-and-roll buoy wave data. *J. Phys. Oceanogr.*, **18**, 1020–1035, doi:10.1175/1520-0485(1988)018<1020:AMFTRA>2.0.CO;2.
- Mei, C. C., 1989: *The Applied Dynamics of Ocean Surface Waves*. Advanced Series on Ocean Engineering, Vol. 1, World Scientific, 768 pp.
- Middleton, F., L. LeBlanc, and M. Czarnecki, 1977: Spectral tuning and calibration of a wave-follower buoy. *J. Pet. Technol.*, **29**, 652–653, doi:10.2118/6280-PA.
- Phillips, O. M., 1985: Spectral and statistical properties of the equilibrium range in wind-generated gravity waves. *J. Fluid Mech.*, **156**, 505–531, doi:10.1017/S0022112085002221.
- Thomson, J., 2012: Wave breaking dissipation observed with “SWIFT” drifters. *J. Atmos. Oceanic Technol.*, **29**, 1866–1882, doi:10.1175/JTECH-D-12-00018.1.
- , E. A. D’Asaro, M. F. Cronin, W. E. Rogers, R. R. Harcourt, and A. Shcherbina, 2013: Waves and the equilibrium range at Ocean Weather Station P. *J. Geophys. Res. Oceans*, **118**, 5951–5962, doi:10.1002/2013JC008837.